# Correspondence

## *Electromagnetic interference in ground-based interferometric radar data from Kronebreen (Svalbard) calving front due to multipath scattering and tidal cycles*

In a recent paper, two of us (Rolstad and Norland, 2009) presented ground-based interferometric velocity measurements from 2007 of Kronebreen (Svalbard) calving front. It is of interest to determine whether the measured glacier velocities are influenced by tides. The intensity of the returned radar signal from the range 4100–4200 m (Fig. 1a; fig. 3 in Rolstad and Norland, 2009) has a sinusoidal pattern, correlated both in time and amplitude with the tidal signal (Fig. 1b). This pattern deserves an explanation. We show here that it is due to destructive interference (canceling the return signal) from multiple path reflections caused by the radar, target and sea-level geometry, and thus is not caused by variations in glacier movement. Radar signals are bounced by the sea surface, and ranges of the pathways between the radar antennas and the reflecting glacier vary according to the tides, and hence sea-level heights. The sinusoidal pattern due to the destructive interference influences neither the measured velocity nor the accuracy of the measurements.

The real-aperture antenna, frequency-modulated continuous-wave interferometric radar operates at 5.75 GHz at a high temporal rate (2 Hz). Velocities can be determined in the radar range direction by tracking natural permanent scatterers on the glacier ice in the radar data. We have not conducted any measurements to determine what surface features act as permanent scatterers, but related studies using ice cores and reflection horizons in firn and superimposed ice measured by ground-penetrating radar at 5.3 GHz are presented by Langley and others (2009), and from glacier ice surfaces using satellite synthetic aperture radar European Remote-sensing Satellite (ERS-1) (5.3 Hz) data by Rees and others (1995). Twenty-three hours of velocity measurements from the period of interest, 29–30 August 2007, at the calving front and also ~147 m further up-glacier are shown in Figure 1c (fig. 4 in Rolstad and Norland, 2009). These results show that the velocities are not clearly influenced by the changes in tidewater sea levels. The velocity ~147 m up-glacier from the front, at range 4189 m, is nearly stable during the period. The speed-up at range 4042 m from 0800 h to 1440 h local time (LT) is thought to be due to rotation of an ice block at the front in advance of calving, as discussed by Rolstad and Norland

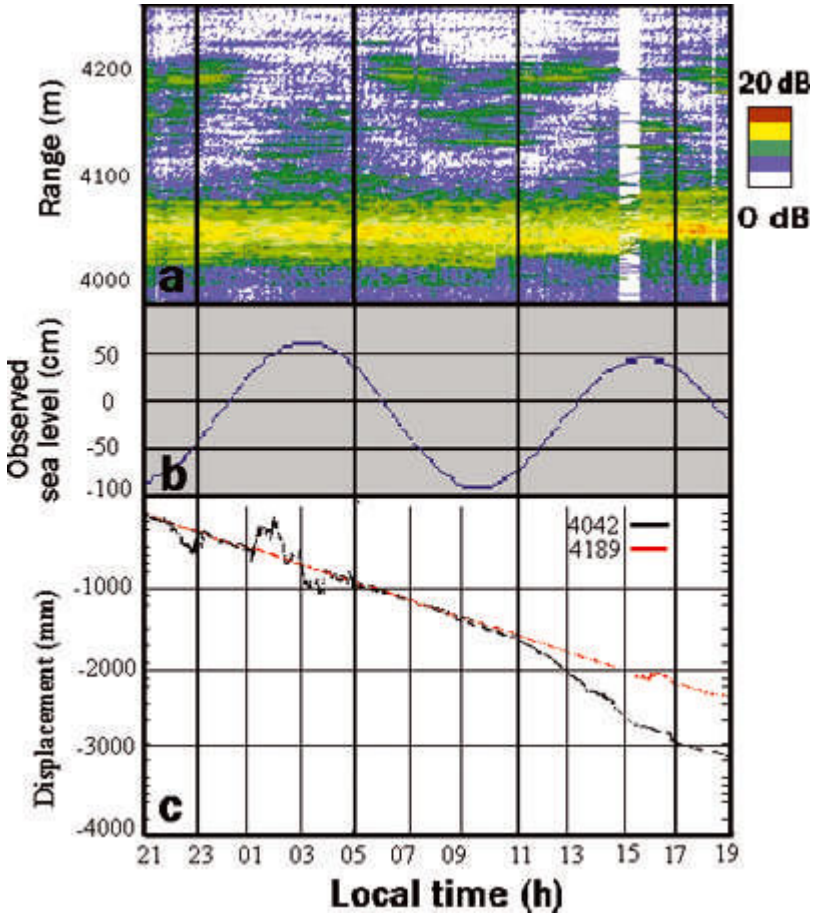


**Fig. 1.** (a) Intensity of returned radar signal (dB), according to the color bar. Range ~4020–4050 m is the vertical glacier front. Sinusoidal-shaped destructive interferometric pattern (white) occurs in range ~4100–4200 m. Measurements from 2100 h LT on 29 August to 1900 h LT on 30 August 2007. (b) Observed sea level in Ny-Ålesund, Svalbard, during the same period, with mean sea level as reference level (Norwegian Hydrographic Service, Norwegian Mapping Authority). (c) Movement profiles in radar range direction at specific ranges, tracked from permanent scatters, 29–30 August 2007, range 4042 and 4189 m.

https://doi.org/10.3189/002214309790152401 Published online by Cambridge University Press

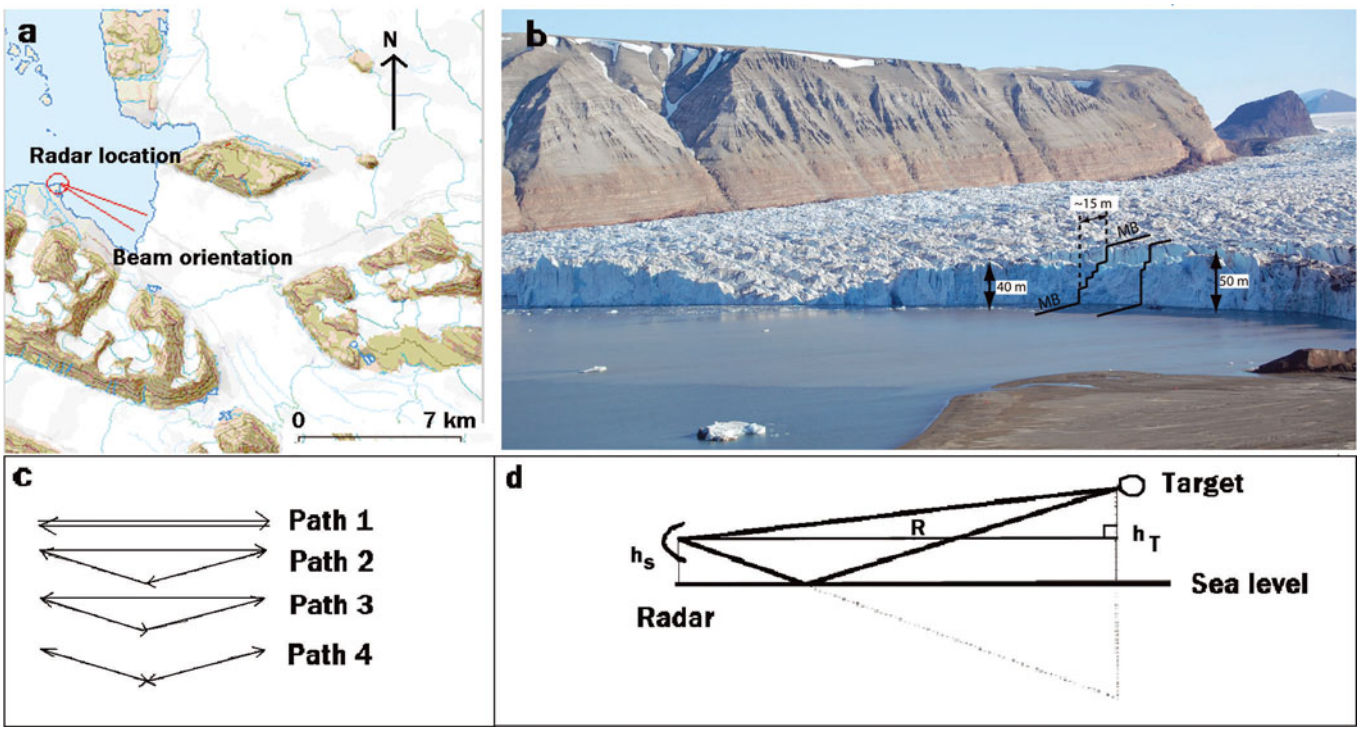


**Fig. 2.** (a) Map showing location of radar and beam orientation during measurements. (b) Monophotogrammetry optical image of glacier calving-front measurement area. MB is main beam location, and black arrows show measured front elevations. The step-like topography near the front is also indicated by black lines. (c) Four possible paths of the radar beam. (d) Geometry of radar, sea surface and reflecting target geometry. $R$ is the range to the scatterer, $h_s$ is the height of the radar antenna and $h_T$ is the height of the point target.

(2009). The main argument for ice-block rotation is that the measured velocities yield surface strain rates, which implies stresses beyond the tensile stress for fracture of ice, and that large transverse surface crevasses are present near the front. However, the movement of the glacier clearly cannot explain the observed sinusoidal pattern in Figure 1a.

## GEOMETRY OF RADAR, SEA-SURFACE AND GLACIER TOPOGRAPHY, AND MULTIPATH REFLECTIONS

During the measurements, the radar antennas are placed ~4 km from the calving front, emitting and receiving directly towards the calving front (Fig. 2a). The radar beam covers a width of ~700 m of the calving front, with the center main beam (MB) position shown in Figure 2b.

In interferometric radar we measure the phase of an electromagnetic wave scattered back from an object at some distance $R$ (the range). The geometry of the reflection path from a target to the receiving radar antenna is shown in Figure 2d. There are four possible paths between antenna and target (Fig. 2c); reflections following paths 1 and 3 go directly between the radar and the target, while reflections following paths 2 and 4 are bounced by the sea surface. Along paths 3 and 4 the beam from the transmitting radar antenna is bounced by the sea surface.

Paths 2 and 3 yield the same path length, while the difference in path length $\Delta d$ between paths 1 and 2 and between paths 3 and 4 can be expressed by a standard approximation (Norland, 2001) as:

$$\Delta d = \frac{2 h_s h_T}{R}, \quad (1)$$

where $h_s$ is the height of the radar antenna and $h_T$ is the height of the point target. A destructive interference pattern will occur when

$$\Delta d = \left(n + \frac{1}{2}\right)\lambda, \quad (2)$$

where $n$ is an integer and $\lambda$ is the electromagnetic wavelength. Both $h_s$ and $h_T$ will vary through the tidal cycle, thus yielding temporal variations in the horizontal distance $R$ to the target giving rise to the destructive interference pattern seen in Figure 1a.

The above equations can be used to determine the distances $R$ at which destructive interferometric patterns may occur for a given target height for $n = 0,1,2,3\ldots$ when $\lambda = 0.056$ m. The height of the radar antenna, $h_s = 5.1$ m a.s.l., was measured using a global positioning system (GPS). The GPS positions are referred to International Terrestrial Reference Frame (ITRF) 2000, and the elevations are ellipsoidal heights corrected with the geoid determined by the Norwegian Mapping Authority. From single-image terrestrial photographs we estimate an average target height near the ice front of $h_T \approx 57$ m (range 4100 m). Applying $n = 0,1,2,3,4\ldots$ we find that the destructive interference pattern may occur at corresponding distances from the radar antenna: $R_{n=0} = 20\,764$ m, $R_{n=1} = 6291$ m, $R_{n=2} = 4152$ m, $R_{n=3} = 2966$ m and $R_{n=4} = 2307$ m. As seen in Figure 1, the range $R \approx 4150$ m for $n = 2$ fits with our estimated geometry.

The slope of the glacier determines the variations in range from ~4100 to ~4200 m, to targets giving rise to the destructive interference pattern during the tidewater cycle. We now evaluate whether the glacier–tidewater-sea-level geometry fits with the observed pattern in Figure 1a. To estimate the height of the reflecting target $h_T$, Equations (1)

https://doi.org/10.3189/002214309790152401 Published online by Cambridge University Press

**Table 1.** Measured antenna heights $h_s$ and ranges $R$ from Figure 1, and calculated target heights $h_T$ for two cycles of tidewater, high and low, for $n = 2$ and $\lambda = 0.056$ m

| Time and sea-level height $h$ | $R$ | $h_s$ | Estimated $h_T$ | Slope |
|---|---|---|---|---|
| | m | m | m | |
| 29 July, 2110 h LT, $h = -0.78$ m | 4100 | 5.88 | 49 | 0.18 |
| 30 Aug., 0330 h LT; $h = 0.72$ m | 4200 | 4.38 | 67 | |
| 30 Aug., 0940 h LT; $h = -0.82$ m | 4100 | 5.92 | 48 | 0.2 |
| 30 Aug., 1550 h LT; $h = 0.54$ m | 4180 | 4.56 | 64 | |

and (2) are solved for $h_T$ using values of $h_s$ corresponding to high and low tide during the cycle, and values of $R$ scaled from Figure 1 for that time. The results are listed in Table 1 for $\lambda = 0.056$ m and $n = 2$. We find that the width of the destructive interferometric pattern requires a fairly steep glacier surface slope. This is consistent with Figure 2b, which shows that the glacier surface topography is steep and 'step-like' in the measurement area. We therefore conclude that the interference pattern in Figure 1 is due to multipath scattering in combination with the geometry of radar, tidewater sea-level and glacier topography, and not a result of movement of the glacier.

*Department of Mathematical Sciences, Norwegian University of Life Sciences, Postboks 5003, NO-1432 Ås, Norway*
*E-mail: cecilie.rolstad@umb.no*
C. ROLSTAD
A. CHAPUIS

*ISPAS AS, Postboks 219, NO-1501 Moss, Norway*
R. NORLAND

*11 September 2009*

## REFERENCES

Langley, K., P. Lacroix, S.-E. Hamran and O. Brandt. 2009. Sources of backscatter at 5.3 GHz from a superimposed ice and firn area revealed by multi-frequency GPR and cores. *J. Glaciol.,* **55**(190), 373–383.

Norland, R. 2001. Multipath scattering from complex targets. *IEE Proc. Radar Sonar Navig.*, **148**(6), 343–347.

Rees, W.G., J.A. Dowdeswell and A.D. Diament. 1995. Analysis of ERS-1 synthetic aperture radar data from Nordaustlandet, Svalbard. *Int. J. Remote Sens.,* **16**(5), 905–924.

Rolstad, C. and R. Norland. 2009. Ground-based interferometric radar for velocity and calving-rate measurements of the tidewater glacier at Kronebreen, Svalbard. *Ann. Glaciol.,* **50**(50), 47–54.

https://doi.org/10.3189/002214309790152401 Published online by Cambridge University Press